

Petrography and geochemistry of the Amphibolites from southeastern part of Yerapalli schist belt, Eastern Dharwar Craton, India

Tushar M Meshram^{*1}, Devasheesh Shukla¹, Kallola K. Behera¹, Satya Narayana Mahapatro², V. Adinarayana Reddy², and K. Chandramouleeswara Rao²

¹Geological Survey of India, Hyderabad, Telangana

²EPMA Laboratory, Geological Survey of India, Hyderabad, Telangana

*Corresponding Author: tusharmeshram1984@gmail.com

ABSTRACT

The Yerapalli schist belt (YSB), predominantly constituted of amphibolites, is considered to be extension of the Nellore-Khammam Schist Belt (NKSB) of the Eastern Dharwar Craton (EDC). Based on field characteristics and fabric elements, two types of amphibolites have been identified in YSB. The NNW-SSE trending older banded and foliated amphibolite associated with metasedimentaries, and the ENE-WSW trending massive amphibolites. Petrographically, the foliated amphibolites consist of amphibole, quartz, plagioclase, chlorite and magnetite, whereas the massive variety is composed of amphibole, plagioclase and chlorite with accessory apatite and titanite. Geochemical studies indicate that the foliated amphibolite enclaves plot in sedimentary field (para-amphibolite), while the massive variety plot in igneous field (ortho-amphibolite). In Niggli c-mg diagram, the ortho-amphibolite indicates characters similar to those of Karroo dolerites, whereas a mixture of pelite-dolomite is observed for para-amphibolite. Similarly, para-amphibolite consist of Mg-rich amphibole and chlorite, while ortho-amphibolite has Fe-rich amphibole and chlorite. In chondrite-normalised REE plots, the ortho-amphibolite shows depleted LREE, with low amplitude positive Eu anomaly while the para-amphibolite exhibits flat REE pattern. This contribution brings out succinct details of field, petrographic mineral chemistry and geochemical charters occurrence of two distinct varieties of amphibolites in the YSB and establishes their igneous and sedimentary parentage.

Key words: Para-amphibolite, Ortho-amphibolite, Yerapalli Schist Belt (YSB).

INTRODUCTION

Amphibolites have found application in elucidating the history of crustal evolution of Precambrian terrains (Graham, 1976; Elueze, 1985; Honkamo, 1987). Leake, 1964 has explained field and geochemical criteria to distinguish between ortho- and para-amphibolites, particularly in high-grade metamorphic terrains. Similar studies can be useful in greenstone belts of the Dharwar craton comprising amphibolites with subordinate metasedimentary and metavolcanics rocks. The prominent greenstone belts of the Eastern Dharwar Craton (EDC) include Kolar, Sandur and Hutti situated near the contact zone with the Eastern Dharwar Craton (WDC), while the Nellore-Khammam schist belt (NKSB) and its extension are exposed along the eastern part of the EDC (Figure 1b) (Jayananda et al., 2000; Bidyananda et al., 2011). These Neoarchean (~2.7 Ga) greenstone belts in the EDC are made up of greenschist to amphibolite facies metabasalts with subordinate komatiites, felsic volcanics and metasediments, BIF, Mg-rich pelites and phyllites (Balakrishnan et al., 1990; Chadwick et al., 2000; Naqvi et al., 2002, 2006; Jayananda et al., 2006; Manikyamba and Khanna, 2007; Rogers et al., 2007; Chardon et al., 2008; Manikyamba and Kerrich, 2012; Dey, 2013).

The Nellore-Khammam Schist Belt (NKSB), is bounded by Proterozoic Eastern Ghat Mobile Belt (EGBM) to east and Proterozoic Cuddapah basin to west (Nagaraja Rao et al., 1987, Vijaykumar et al., 2006; Chetty, 1999; Sesha Sai, 2013). It has been divided into older low-grade metasedimentary rocks, occurring in southwestern part and younger high-grade metabasic rocks in the eastern part (Okudaria et al., 2000 and Hari Prasad et al., 2000). According to them amphibolites of the NKSB show modern oceanic arc and continental arc basalt affinities. According to Vijay Kumar et al., (2006) and Saravothaman (1995), these amphibolites are tholeiitic in nature and compositionally similar to Fe-rich mafic rocks of other greenstone belts of the EDC.

The present study area i.e. the NNW-SSE striking Yerapalli schist belt (YSB) is ~40-50 km long with varying width from 20 m – 200 m and is considered to be an extension of the NKSB. Amphibolites of two distinct varieties occur in the area. One variety of amphibolite is banded and foliated in nature and occur as elongated mega enclaves associated with Banded Magnetite Quartzite (BMQ), quartzite and biotite-sericite schist in granitoids. The other amphibolite is massive in nature and occurs as ENE-WSW trending metamorphosed basic intrusive bodies, which are exposed over a stretch of 8-10 km length and

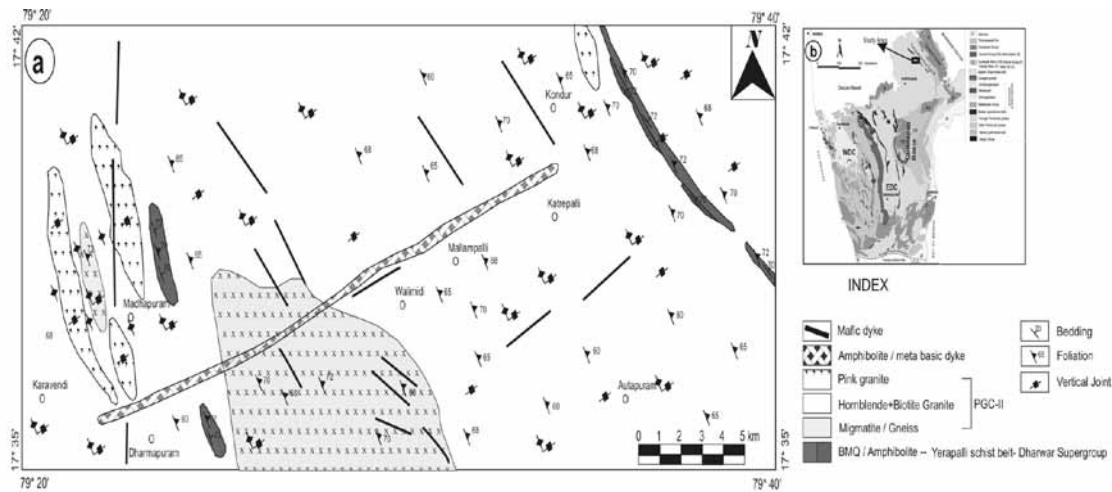


Figure 1. a) Geological map of the area around Madhapuram-Walimidi-Autapuram. b) Geological map of Dharwar Craton (adapted from project Vasundhara map of GSI, 1994).

100 m width. Previous workers have suggested igneous parentage for the amphibolites of the NKSB. Present study reveals the sedimentary parentage for the foliated variety of amphibolite and igneous parentage for the massive type of amphibolite. In this contribution, we describe their field relationship, and mineralogically and geochemically characterize the para- and ortho-amphibolites of the YSB. Further we emphasize on petrogenesis of the two amphibolite types.

Geological setting and field relationship:

Elongated to lenticular bands of BIF, amphibolite, quartzite, mica-schist belonging to the YSB and migmatite occur as enclaves/xenoliths within hornblende+biotite gneisses occupying most of the study area. This is intruded by granite of Peninsular Gneissic Complex (PGC-II) (Figure 1) with younger mafic dykes. Field studies reveal two types of amphibolites on the basis of their texture, structure and mineralogy. These include NNW-SSE trending foliated/banded amphibolite and ENE-WSW trending non-foliated/massive amphibolite. The foliated amphibolites are associated with BMQ, garnetiferous quartzite and schists of the YSB. These occur as enclave/xenolith within gneisses. These exhibit gradational contact with garnetiferous quartzite (Figure 2g). Thin bands of quartzite alternate with foliated amphibolite (Figure 2 a and b) exhibiting banded appearance. The massive amphibolite (hereafter ortho-amphibolite) occurs as metamorphosed basic intrusive within the gneiss and granite. The field characters of foliated amphibolite (hereafter para-amphibolite) suggests its sedimentary parentage. Structurally para-amphibolite shows imprints of polyphase deformation with development of three different generation of folds i.e., F_1 , F_2 and F_3 (Figure 2 a and b) but ortho-amphibolite is undeformed (Figure 2 c and d).

Analytical technique: Whole-rock major and trace element analyses were carried out at the Chemical Laboratory, GSI, Hyderabad. The XRF spectrometry was used to analyze major oxide, whereas ICP-MS (Model: Perkin Elmer Sciex ELAN 600) was used to determine trace and REE concentration. Mineral chemistry was obtained by EPMA (CAMECA SX-100) at GSI, Southern Region, Hyderabad. A beam of $1\mu\text{m}$ diameter was used with an accelerating voltage of 20 kV and beams current of 15 nA for sulphides and 15 kV voltage / 12nA beam current for silicates and oxides. Natural standards were used for all elements except Mn and Ti for which synthetic standards were used.

Petrography and mineral chemistry

Para-amphibolites: These are fine- to medium-grained with well developed mafic and felsic mineral banding (Figure 2a). It shows granoblastic texture and composed of amphibole (65%), plagioclase (20%), quartz (10%), chlorite (2.5%), epidote (1.5%), and magnetite (0.5%) (Figure 2c). Amphiboles show preferred alignment defining foliation in the rock. The associated quartzite is medium- to coarse-grained and mainly consist of quartz along with minor plagioclase and garnet (Figure 2h). The quartz grains show recrystallization due to later deformation. The plagioclase grains show polysynthetic twinning and are partially altered (Figure 2h). Amphiboles are compositionally actinolite-hornblende to magnesio-hornblende in $\text{Mg}/\text{Mg} + \text{Fe}^{2+}$ vs TSi diagram (Leake et al., 1997) (Figure 3a) (Table 4). Plagioclase is mostly oligoclase to labradorite ($\text{An}_{22.3-57.9}$) (Figure 3d). At places quartz, epidote and plagioclase occur interstitial to hornblende grains. The chlorite occurs as alteration product of hornblende having restricted range of MgO (23.46-22.19 wt%) and FeO (15.89-15.14 wt%) and plot within overlapping field of ripidolite and pycnochlorite field (Figure 3c) (Table 5).

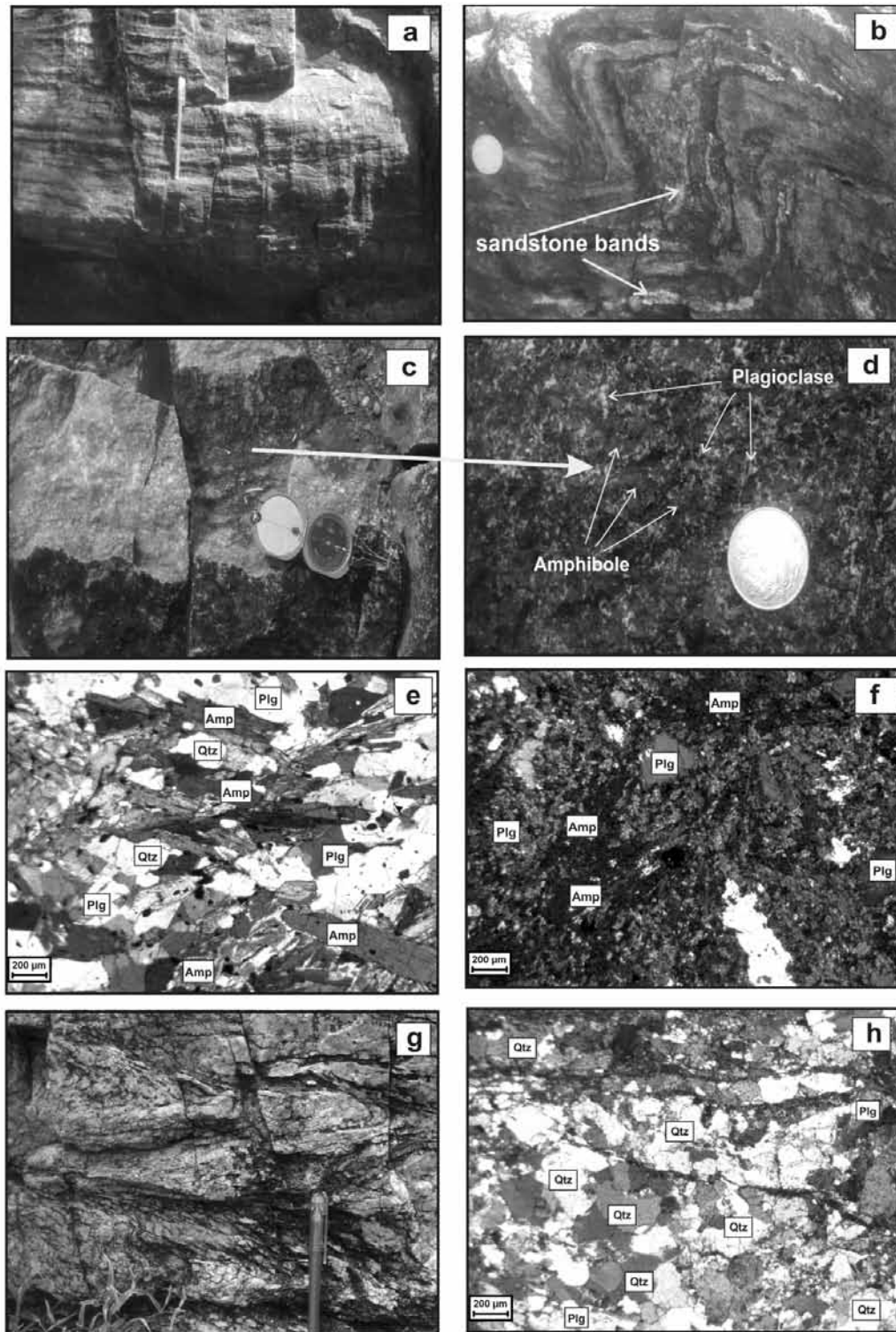


Figure 2. Field photograph of Amphibolite of YSB. a) Shows banded nature of NNW-SSE trending para amphibolite. b) Development of folds in para amphibolite with intercalation of sandstone layers. c) Outcrop pattern of ENE-WSW trending massive ortho amphibolite. d) Distribution of amphiboles and plagioclase minerals in ortho amphibolite. e) Photomicrograph shows two sets of alignment of amphiboles in para amphibolites. f) Photomicrograph shows alteration of amphibole to chlorite and plagioclase to epidote within ortho amphibolite. g) Field photograph shows deformed and sheared garnetiferous quartzite with primary bedding plane along with development of intrafolial F1 folds. h) Photomicrograph shows quartzite.

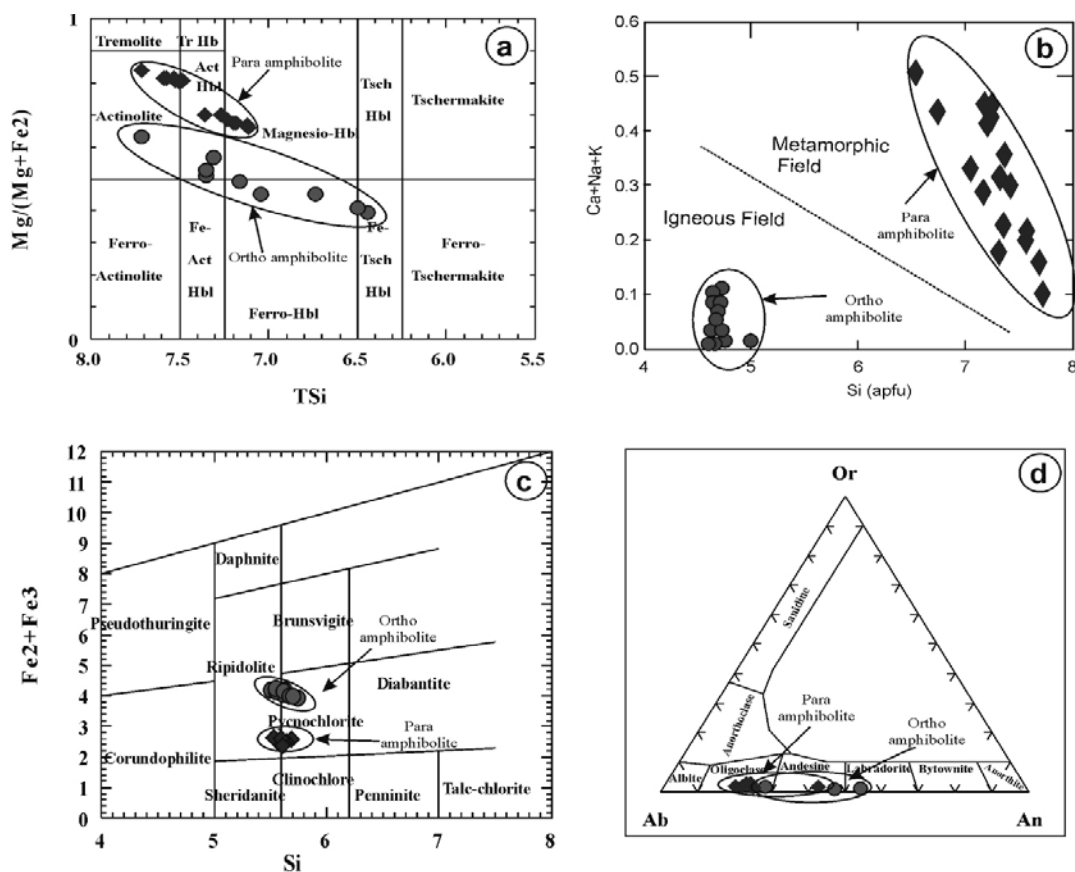


Figure 3. a) Nomenclature of amphibole after Leake (1977), b) Compositional variations of amphibole from the two different amphibolites, plotted in terms of cations (Ca+Na+K) vs Si (apfu) diagram after Giret et al., 1980, c) Nomenclature and classification of chlorite after Hey, 1954, d) Nomenclature and classification of feldspar.

Ortho amphibolites: These are medium- to fine-grained and massive in nature (Figure 2b). They are made up of amphibole (60%), plagioclase (35%) and accessory phases (5%) such as epidote, chlorite, ilmenite, apatite and sphene. Amphibole grains are subhedral and contain plagioclase and ilmenite as inclusions. Most of the amphiboles are chloritised and plagioclase is saussuritised. Following the classification of Leake et al., (1997), amphiboles are actinolite, Fe hornblende to Fe tschermakite (Figure 3a) and plagioclases are oligoclase to andesine (An 28.3 – 58.9%) composition (Figure 3d). Chlorites with MgO (18.40% -16.82%) and FeO (23.50% to 21.93%) contents plot within overlapping fields of ripidolite and pycnochlorite (Figure 3c).

Geochemistry of Amphibolites:

Whole-rock major oxide, trace element and REE data for selected representative samples of both amphibolite types are presented in Table 1, 2 and 3. Standardized Niggli for all samples were automatically computed using the GCD kit.

Para-amphibolite: Geochemically, para-amphibolites have moderate SiO₂ (58.80-48.67%), Al₂O₃ (14.66-09.08%), Fe₂O₃^T (26.94-13.25), higher CaO (09.96-0.32%), MgO (5.92-0.10%) range and lower MnO, Na₂O, TiO₂, K₂O,

P₂O₅ contents. These are enriched in alumina and silica but depleted in iron and CaO which suggest their sedimentary protolith character. In Na₂O/Al₂O₃ vs. K₂O/Al₂O₃ diagram (Garrels and Mackenzie, 1971) and Na₂O+K₂O vs. 100*K₂O/Na₂O+K₂O variation diagram (Honkamo, 1987) (Figure 4b and 4c), these samples plot in sedimentary field, suggesting their sedimentary parentage. In Niggli c-mg diagram which is commonly used to distinguish between ortho- and para-amphibolites, para-amphibolite samples plot in fields of limestone mixture and pelite-dolomite mixture (Figure 5a and b). In c-(al-alk)-100 mg diagram of Leake, 1964 some para-amphibolite samples plot away but nearer to dolomite and pelite-semipelite fields (Figure 5c). Various bivariate plots also indicate sedimentary precursors for para-amphibolites. They are inferred to have formed by metamorphism of calcareous and/or dolomitic pelites. The occurrence of the amphibolites in association with thin bands of quartzite further strengthens their metasedimentary nature.

Ortho-amphibolite: Geochemically, ortho-amphibolites show moderate range of SiO₂ (54.74-49.96%), Al₂O₃ (11.54-10.58%), Fe₂O₃^T (16.07-13.25%), CaO (10.76-5.91%), MgO (5.38-3.39%) and lower MnO, Na₂O, TiO₂, K₂O, P₂O₅ contents. These are sub-alkaline in nature for ortho amphibolites (Irvine and Barager, 1971)

Petrography and geochemistry of the Amphibolites from southeastern part of Yerapalli schist belt, Eastern Dharwar Craton, India

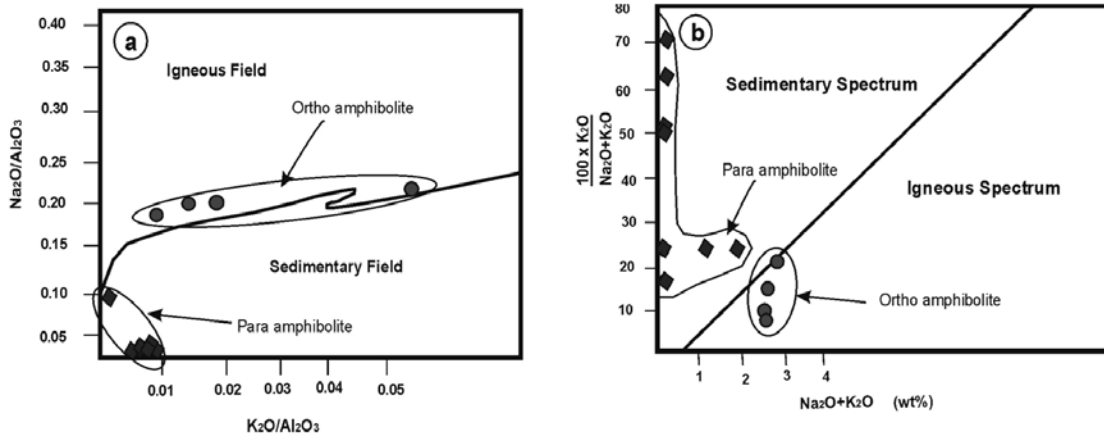


Figure 4. a) Na₂O/ Al₂O₃ Versus K₂O/ Al₂O₃ for Yerapalli amphibolites (Garrels, and Mackenzie, 1971). b) Na₂O + K₂O versus 100x K₂O / Na₂O + K₂O of Yerapalli amphibolites and other comparable rocks (Honkamo, 1987).

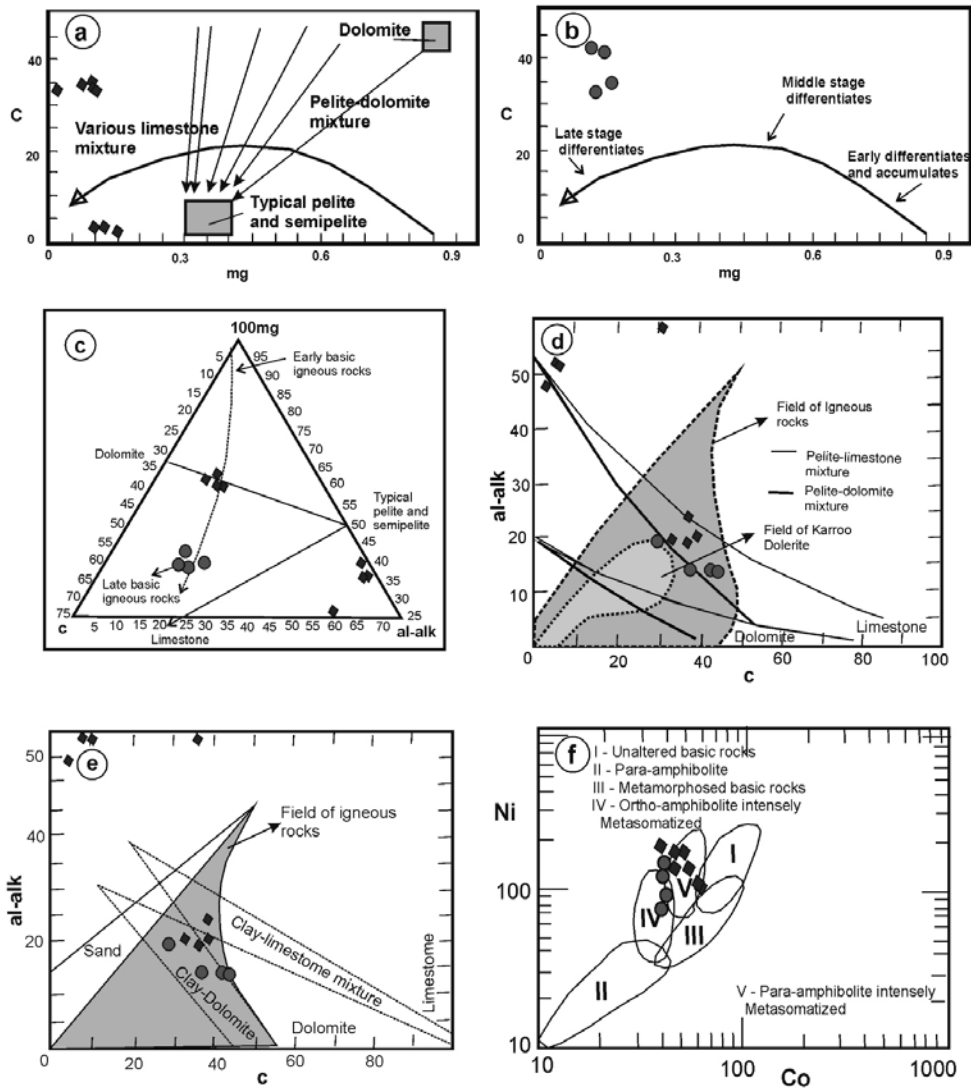


Figure 5. Variation diagram for the studied amphibolites: a & b) Niggli c vs. Mg (Leake, 1964), c) Niggli c-Mg-(Al-alk) ternary diagram (Leake, 1964), d) Plot of Niggli values (al-alk) (Evans & Leake, 1960). e) Niggli c vs. al-alk (Leake and Singh 1986), f) Plot of Ni vs. Co, respectively (Walker et al., 1960).

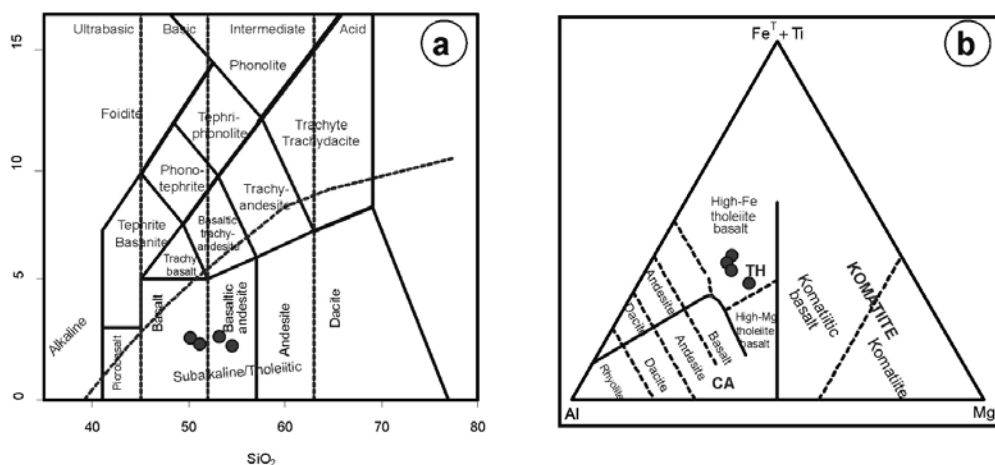


Figure 6. a) $\text{Na}_2\text{O}+\text{K}_2\text{O}$ versus SiO_2 discrimination diagram of Le Bas et al., (1979), showing the basaltic nature of the massive amphibolites. b) Ternary plot of classification according to cation percentage of Al, (Fe total+ Ti) and Mg after Jensen, (1976).

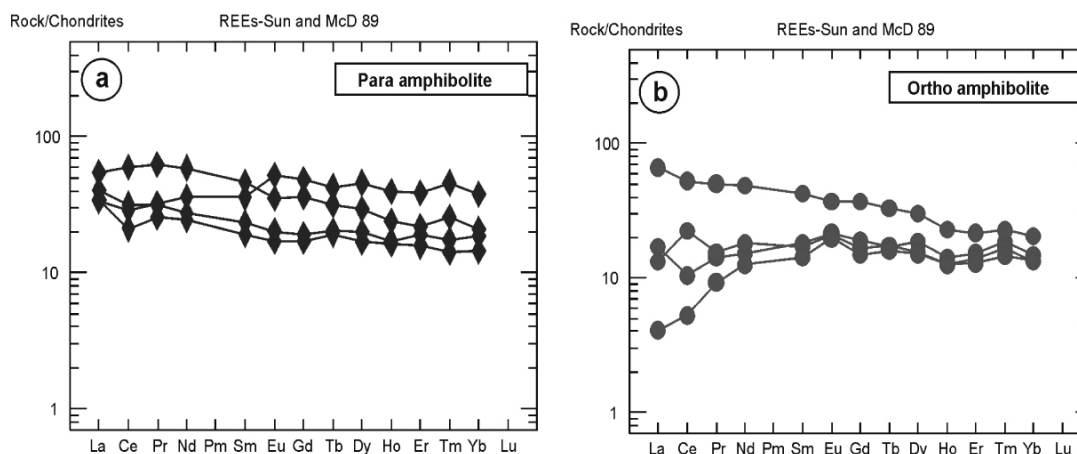


Figure 7. Chondrite normalized rare earth element patterns of a) Para amphibolites and b) Ortho amphibolites. Normalizing constants after, Sun and McDonough (1989).

(Figure 6a). In $\text{Na}_2\text{O}/\text{Al}_2\text{O}_3$ vs. $\text{K}_2\text{O}/\text{Al}_2\text{O}_3$ diagram (Garrels and Mackenzie, 1971) and $\text{Na}_2\text{O}+\text{K}_2\text{O}$ vs. $100 \cdot \text{K}_2\text{O}/\text{Na}_2\text{O}+\text{K}_2\text{O}$ diagram (Honkamo, 1987) (Figure 4a and 4b), samples of ortho-amphibolite plot in igneous field suggesting their igneous protolith character. Similarly, in Niggli c-mg diagram (Figure 5a and b) ortho-amphibolites plot along the Karoo dolerite trend (Figure 5d and 5e). In c-(al-alk)-100 mg diagram of Leake 1964, these samples plot as on or close to the late basic igneous rocks (Figure 5c).

All samples of ortho-amphibolite confirm their likely protoliths to be tholeiite basalts as indicated from SiO_2 vs. $\text{Na}_2\text{O} + \text{K}_2\text{O}$ plot of Le Bas et al., 1986 (Figure 6a) and $\text{Fe}+\text{Ti} - \text{Al} - \text{Mg}$ diagram of Jensen, 1976 (Figure 6b). Further, the above discussions indicate that the older para amphibolites are derived from sedimentary environment and younger ortho-amphibolite are derived from magmatic basic rocks. All the amphibolite samples have low total REE content and lack any kind of typical LREE and HREE fractionation pattern. However, ortho-amphibolite samples

are depleted in LREE with small positive Eu anomaly and flat HREE (Figure 7b) similar to basic rocks, while para-amphibolite samples have nearly flat REE fractionation pattern with no Eu anomaly (Figure 7a).

Discussion: Leake (1964) proposed geological and geochemical approach to known igneous and sedimentary parentage for amphibolites. Though the nature of primary source material gets blurred in a polymetamorphic environment, the amphibolites retain their chemical inheritance during metamorphism due to presence of lesser mobile chemical components, like Fe, Mg, Ti, etc. (Miyashiro, 1973). Further, Leake (1964) suggested the meta-igneous amphibolite to be completely re-crystallized dolerites, basalt or basic tuffs and para-amphibolites to be equivalents of carbonate (calcite or dolomite) mixed pelitic sediments. Leake (1964), Evans and Leake (1960), Gate (1967), and Van de Camp (1969) have demonstrated the effective use of Niggli values in distinguishing ortho-amphibolites and para-amphibolites. Although no single

Petrography and geochemistry of the Amphibolites from southeastern part of
Yerapalli schist belt, Eastern Dharwar Craton, India

Table 1. Representative major oxide analysis of amphibolites.

	Para Amphibolites (Banded)								Ortho Amphibolites (Massive)			
	L-242A	L-242B	L-212	L-264	L-215	L-238	L-281A	L-283	L-276B	L-281	L-289	L-290
SiO ₂	53.90	55.45	53.25	53.99	48.67	56.74	58.80	54.57	52.68	54.74	51.29	49.96
Al ₂ O ₃	14.66	13.50	9.93	10.93	12.57	10.68	9.08	9.45	11.54	11.24	10.58	10.71
Fe ₂ O ₃ ^T	15.95	15.41	21.06	15.67	26.94	16.36	13.31	14.14	13.25	16.07	13.55	14.20
MnO	0.19	0.19	0.18	0.21	0.19	0.23	0.47	0.11	0.19	0.34	0.19	0.20
MgO	3.50	3.64	5.82	4.23	0.10	2.68	5.92	5.44	5.38	3.96	3.75	3.39
CaO	0.95	0.93	0.32	8.84	3.74	6.92	6.96	9.16	10.49	5.91	10.76	10.77
Na ₂ O	0.10	0.10	0.16	1.77	0.05	1.15	0.31	0.34	2.08	2.11	2.22	2.07
K ₂ O	0.10	0.10	0.05	0.49	0.10	0.34	0.88	0.07	0.69	0.22	0.15	0.41
TiO ₂	0.69	0.72	1.37	1.04	0.85	1.14	0.77	0.98	0.73	1.23	0.78	0.81
P ₂ O ₅	0.02	0.01	0.13	0.19	0.15	0.12	0.11	0.16	0.10	0.17	0.11	0.11
total	90.06	90.05	92.27	97.36	93.36	96.36	96.61	94.42	97.13	95.99	93.38	92.63
Niggli Values												
C	6.698	6.779	2.254	38.779	33.854	38.557	32.574	40.961	39.193	29.683	44.75	45.535
al	56.849	54.119	38.472	26.37	62.579	32.728	23.372	23.241	23.713	31.048	24.2	24.904
fm	35.395	38	58.045	26.546	2.619	21.789	40.289	34.235	28.528	29.023	22.324	20.61
alk	1.058	1.093	1.229	8.305	0.948	6.925	3.765	1.562	8.566	10.246	8.725	8.951
al-alk	55.791	53.026	37.243	18.065	61.631	25.803	19.607	21.679	15.147	20.802	15.475	15.953
mg	0.098	0.105	0.120	0.118	0.002	0.075	0.179	0.160	0.167	0.108	0.120	0.105
100*mg	9.83	10.505	12.094	11.822	0.184	7.521	17.933	16.080	16.775	10.867	12.081	10.597

The comparative characteristic of both amphibolites are summarized as follows.

	Para amphibolite	Ortho amphibolite
Mineralogy	Amphibole (65%), plagioclase (20%), quartz (10%), chlorite (2.5%), epidote (1.5%), and magnetite (0.5%)	Amphibole (60%), plagioclase (35%) and epidote+apatite+sphene+ilmenite (5%)
Amphibole Plagioclase Chlorite	Actinolite-Hornblende to Magnesio-hornblende oligoclase to labradorite ripidolite and pycnochlorite MgO (23.464% -22.195%) and FeO- (15.898% to 15.143 %)	Actinolite – Fe hornblende to Fe –tschermakite oligoclase to andesine ripidolite and pycnochlorite MgO (18.402% -16.829%) and FeO- (23.507% to 21.934 %)
Geochemistry	SiO ₂ 58.80 - 48.67%, Al ₂ O ₃ 14.66 - 09.08%, Fe ₂ O ₃ ^T 26.94 – 13.25%	SiO ₂ 54.74 - 49.96%, Al ₂ O ₃ 11.54 - 10.58%, Fe ₂ O ₃ ^T 16.07 – 13.25%
Structure	Strongly deformed, shows 3 phases of deformation.	Massive and undeformed nature only with fracture
Fabric	Highly foliated and banded in nature shows NNW-SSE regional trend	Shows ENE-SWS trend
Remarks	1) Derivative of metamorphosed sedimentary rocks (carbonate-pelites) 2) It is part of YSB, (extension of NKSB).	1) Derivative of metamorphosed magmatic/igneous rocks (Fe-tholeiite) 2) It is younger intrusive metabasic dyke.

change in the amount of a major element is uniquely associated with magmatic differentiation or sedimentary variation, the systematic decrease in Niggli Mg [Mg= MgO / (FeO+MnO+2Fe₂O₃+MgO)] and fm with increase in si, alk, al and ti is commonly associated with magmatic differentiation in basic magmas, while opposite condition is present in pelite-dolomite mixture.

Geochemical studies indicate that the foliated amphibolite enclaves plot in sedimentary field (para-amphibolite), while the massive variety plot in igneous field (ortho-amphibolite). The Si vs. Na+K+Ca plot of amphiboles (Giret, et al., 1980) (Figure 3b) discriminate them in igneous and metamorphic field. Chondrite normalised REE pattern, especially behavior of Eu anomaly,

Table 2. Representative trace element analysis of amphibolites.

	Para Amphibolites							Ortho Amphibolites			
	L-242A	L-242B	L-212	L-264	L-215	L-238	L-281A	L-276B	L-281	L-289	L-290
Be	-	-	0.21	0.71	0.60	0.99	-	0.67	1.03	0.43	0.50
Ge	-	-	1.01	1.90	1.12	1.28	-	1.88	2.01	1.66	1.31
Nb	-	-	5.00	5.00	6.13	5.00	-	5.00	13.27	5.00	5.00
Mo	-	-	5.00	5.00	5.00	5.00	-	5.00	5.00	5.00	5.00
Sn	-	-	5.00	5.00	5.00	5.00	-	5.00	5.00	5.00	5.00
Hf	-	-	4.48	3.54	2.85	2.27	-	1.39	3.45	1.28	0.43
Ta	-	-	0.27	0.41	0.29	0.43	-	0.15	0.83	0.17	0.08
Bi	-	-	0.41	0.10	0.33	0.10	-	0.10	0.10	0.10	0.10
U	-	-	5.00	5.00	5.00	5.00	-	5.00	1.00	5.00	5.00
Ba	203	238	182	200	207	208	193	195	196	199	199
Ga	10	8.4	<5	12	12	9.4	5.0	7.6	10	9.5	6.5
Sc	84	77	226	31	23	13	10	<3.5	39	<3.5	4.9
V	389	378	580	239	260	314	216	251	292	249	263
Th	12	8.8	<4	<4	<4	<4	12	<4	<4	<4	<4
Pb	<2	<2	<2	<2	9.3	<2	<2	<2	26	8.6	4.9
Ni	108	109	169	190	147	135	160	178	78	162	169
Co	63	61	57	38	53	43	45	46	48	46	45
Rb	5.1	5.6	16	83	25	7.4	5.8	14	19	17	48
Sr	38	38	41	67	100	239	124	100	88	145	128
Y	<5	<5	<5	13	6.6	5.1	<5	7.1	6.5	<5	5.4
Zr	68	68	97	75	89	96	105	41	101	54	45
Nb	6.4	5.7	9.3	13	6.1	5.0	8.7	7.5	9.0	<5	5.1
Cr	146	141	137	398	94	148	71	234	92	203	211
Cu	1.1	<1	336	51	193	255	3.2	5.2	135	190	94
Zn	74	78	107	81	79	28	30	73	100	70	90

Table 3. Representative rare earth element analysis of amphibolites.

	Para Amphibolite				Ortho Amphibolite			
	L-212	L-281A	L-264	L-283	L-276B	L-281	L-289	L-290
La	8.02	12.85	9.56	8.24	4.01	15.78	3.14	0.96
Ce	17.79	36.31	19.47	12.92	6.39	32.15	13.65	3.21
Pr	3.04	5.91	2.98	2.43	1.35	4.78	1.46	0.88
Nd	16.76	27.55	12.92	11.43	7.07	22.71	8.44	5.84
Pm	-	--	--	--	--	--	--	--
Sm	5.48	7.16	3.58	2.93	2.77	6.49	2.61	2.18
Eu	3.03	2.03	1.17	0.98	1.25	2.14	1.21	1.15
Gd	9.91	7.49	3.92	3.48	3.92	7.61	3.44	3.03
Tb	1.60	1.19	0.76	0.72	0.64	1.23	0.65	0.60
Dy	11.65	7.45	5.10	4.30	4.71	7.63	3.97	3.83
Ho	2.25	1.35	0.97	0.92	0.80	1.29	0.71	0.72
Er	6.41	3.58	3.17	2.60	2.53	3.55	2.30	2.12
Tm	1.17	0.65	0.44	0.36	0.47	0.58	0.42	0.37
Yb	6.41	3.55	3.14	2.48	2.51	3.46	2.25	2.28
Lu	0.94	0.59	0.44	0.39	0.36	0.50	0.36	0.34
LREE	54.12069	91.81435	49.68938	38.9374	22.83709	84.0478	30.51028	14.22568
HREE	40.34147	25.84676	17.94782	15.24791	15.93904	25.85479	14.09841	13.30561
TREE	94.46216	117.6611	67.63719	54.18532	38.77614	109.9026	44.6087	27.5313

also reveals the nature of origin of amphibolites. The ortho-amphibolite exhibit small positive Eu anomaly and flat HREE (Figure 7b) similar to basic rocks, while the para-amphibolite samples have nearly flat REE fractionation pattern with no Eu anomaly (Figure 7a). The genetic aspect of amphibolite of the YSB was not discussed earlier (Babu, 2001). Geological, geochemical and mineral chemical characters clearly suggest that the amphibolite of the YSB represent metamorphosed equivalents of calcareous and/or dolomitic pelites and have a sedimentary parentage. Further, the chemical characters of ortho-amphibolite can be compared with those of other schist belt of EDC (Okudaria et al., 2000; Hari Prasad et al., 2000; Vijaykumar et al., 2006; Sarvothman, 2001); Rajasthan (Thomas and Paudel, 2015); Jharkhand (Pandey, et al., 2013).

CONCLUSION

The present study conclusively establishes sedimentary parentage for the amphibolites of the YSB based on their field, petrographic, mineral chemical and geochemical characters. The massive amphibolites occurring in the granite are metamorphosed basic intrusives having igneous parentage. The geochemical characters and mineral chemistry highlight these differences and help to distinguish their protolith character. The NNW-SSE trending banded para-amphibolite of the YSB are older to the intrusive granitoids as well as the ENE-WSW trending ortho-amphibolite.

ACKNOWLEDGMENTS

The authors thank Shri. B. D. Thappa; (Additional Director General), Shri. P. A. Ramesh Babu; (Deputy Director General) and Director Publication Division, GSI, Hyderabad, India for the publication approval of this research paper. Dr. G. Suresh, Shri. Anil Kumar and Shri. Bibin Das, GSI, Southern Region, Hyderabad are profusely thanked for their help during petrographic studies. Dr. V.V. Sesha Sai (Editorial Board Member and reviewer; GSI, Hyderabad), Dr. Rajkumar Meshram (GSI, Nagpur) and Dr. K.V.S Subrahmaniyam and Dr. S. Sawant (NGRI, Hyderabad) are gratefully acknowledged for their valuable suggestions, comments and discussion which greatly helped to improve the manuscript. Thanks are due to Chief Editor for his kind support & encouragement.

Compliance with Ethical Standards

The authors declare that they have no conflict of interest and adhere to copyright norms.

REFERENCES

Babu, V.R.M., 2001. Plate Tectonic History of the Indian Plate Nellore Khammam Schist Belt, Indian Academy of Geoscience, v.183.

- Balakrishnan, S., Hanson, G.N., and Rajamani, V., 1990. Pb and Nd isotope constraints on the origin of high Mg and tholeiitic amphibolites, Kolar schist belt, southern India, *Contribution to Mineralogy and Petrology*, v.107, pp: 279-292.
- Bidyananda, M., Goswami, J.N., and Srinivasan, R., 2011. Pb-Pb zircon ages of Archaean metasediments and gneisses from the Dharwar craton, southern India: implications for the antiquity of the eastern Dharwar craton, *Journal of Earth System Science*, v.120, pp: 643-661.
- Chadwick, B., Vasudev, V.N., and Hegde, G.V., 2000. The Dharwar craton, southern India, interpreted as the result of Late Archaean oblique convergence, *Precambrian Research*, v.99, pp: 91-111.
- Chardon, D., Jayananda, M., Chetty, T.R.K., and Peucat, J.-J., 2008. Precambrian continental strain and shear zone patterns: South Indian case. *Journal of Geophysical Research – Solid Earth*, pp: 113.
- Chetty, T.R.K., 1999. Some observations on the tectonic framework of Southeastern Indian Shield. *Gondwana Res.*, v.2, pp: 651-653.
- Dey, S., 2013. Evolution of Archaean crust in the Dharwar craton: the Nd isotope record. *Precambrian Research*, v.227, pp: 227-246.
- Elueze, A.A., 1985. Petrochemical and petrogenetic characteristics of Precambrian amphibolites of the Alawa District, NW Nigeria. *Chem. Geol.*, v.48, pp: 29-41.
- Evans, B.W., and Leake, B.E., 1960. The composition and origin of striped amphibolites of Connemara, Ireland. *Journal of petrology*, v.1, pp: 337-363.
- Garrels, R.M., and Mackenzie, F.F., 1971. Evolution of sedimentary rocks. W.M. Noron and Co., New York, p: 394.
- Gates, R.M., 1967. Amphibolites - Syntectonic Intrusives. *Am. J. Sci.*, v.265, pp: 118-131.
- Giret, A., Bonin, B., and Léger, J.M., 1980. Amphibole compositional trends in oversaturated and undersaturated alkaline plutonic ring complexes. *Canadian Mineralogist*, v.18, pp: 481-495.
- Graham, C.M., 1976. Petrochemistry and tectonic significance of Daldrian metabasaltic rocks of the SW Scottish Highlands. *J. Geol. Soc. Lond.*, v.132, pp: 61-84.
- Hari Prasad, B., Okudaira, T., Hayasaka, Y., Yoshida, M., and Divi, R.S., 2000. Petrology and Geochemistry of Amphibolites from the Nellore-Khammam Schist Belt, SE India. *Journal of Geol. Soc. India*, v.56, no.1, pp: 67-78.
- Honkamo, M., 1987. Geochemistry and tectonic setting of early Proterozoic volcanic rocks in Northern Oshuthotria Finland, In: Pharaoh TC Beckingsale RD Richard D. (Eds.) *Geochemistry and mineralisation of Proterozoic volcanic suites. Geol. Soc. Spec. Publ.*, v.38, pp: 231.
- Hey, M.H., 1954. A new review of the chlorites. *Mineral. Mag.* v.30, pp: 277-292.
- Irvine, T.N., and Baragar, W.R.A., 1971. A guide to the chemical classification of the common volcanic rocks. *Can J Earth Sci.*, v.8, pp: 523-548.
- Jayananda, M., Moyen, J.-F., Martin, H., Peucat, J.-J., Auvray, B., and Mahabaleshwar, B., 2000. Late Archean (2550–2520 Ma) juvenile magmatism in the Eastern Dharwar Craton, Southern India: constrains from geochronology, Nd–Sr

- isotopes and whole rock geochemistry. *Precambrian Research*, v.99, pp: 225-254.
- Jayananda, M., Chardon, D., Peucat, J.-J., and Capdevila, R., 2006. 2.61 Ga potassic granites and crustal reworking in the western Dharwar craton, southern India: tectonic, geochronologic and tectonic constraints. *Precambrian Research*, v.150, pp: 1-26.
- Jensen, L.S., 1976. A new cation plot for classifying subalkalic volcanic rocks. *Ontario Div. Mines. Misc. Pap.*, p: 66.
- Leake, B.E., 1964. The chemical distinction between ortho- and para-amphibolites. *J. Petrol.*, v.5, pp: 238-254.
- Leake, B.E., Woolley, A.R., Arps, C.E.S., Birch, W.D., Gilbert, M.C., Grice, J.D., Hawthorne, F.C., Kato, A., Kisch, H.J., Krivovichev, V.G., Linthout, K., Laird, J., Mandarino, J., Maresch, W.V., Nickel, E.H., Rock, N.M.S., Schumacher, J.C., Smith, D.C., Stephenson, N.C.N., Ungaretti, L., Whittaker, E.J.W., and Youzhi, G., 1997. Nomenclature of amphiboles: Report of the subcommittee on amphiboles of the International Mineralogical Association Commission on New Minerals and Mineral Names". *Canadian Mineralogy*, v.35, pp: 219-246.
- Leake, B.E., and Singh, D., 1986. The Delaney Dome formation, Connemara, W. Ireland and the geochemical distribution of ortho- and para-quartzofeldspathic rocks. *Mineral Mag*, v.50, pp: 205-215.
- Le Bas, M.J., Le Maitre, R.W., Streckeisen, A., and Zanettin, B., 1986. A chemical classification of volcanic rocks based on total alkali-silica diagram. *Journal of Petrology*, v.27, pp: 745-750.
- Manikyamba, C., and Khanna, T.C., 2007. Crustal growth processes as illustrated by the Neoproterozoic intraoceanic magmatism from Gadwal greenstone belt, Eastern Dharwar Craton, India. *Gondwana Research*, v.11, pp: 476-491.
- Manikyamba, C., and Kerrich, R., 2012. Eastern Dharwar Craton, India: continental litho-sphere growth by accretion of diverse plume and arc terranes. *Geoscience Frontiers*, v.3, pp: 225-240.
- Miyashiro, A., 1973. *Metamorphism and metamorphic belts*. George Allen and Unwin. London., pp: 493.
- Nagaraja Rao, B.K., Rajurkar, S.T., Ramalingaswamy, G., and Ravindra Babu, B., 1987. Stratigraphy, structure and evolution of the Cuddapah basin. In: Radhakrishna, B.P. (Ed.), *Purana Basins of Peninsular India (Middle to Late Proterozoic)*, Geological Society of India Memoirs, v.6, pp: 33-86.
- Naqvi, S.M., Manikyamba, C., Ganeshwara Rao, T., Subba Rao, D.V., Ram Mohan, M., Srinivasa and Rama, D., 2002. Geochemical and isotopic constraints of Neoproterozoic fossil plume for evolution of volcanic rocks of Sandur greenstone belt, India. *Journal Geological Society of India*, v.60, pp: 27-56.
- Naqvi, S.M., Khan, R.M.K., Manikyamba, C., Ram Mohan, M., and Khanna, T.C., 2006. Geochemistry of the Neoproterozoic high-Mg basalts, boninites and adakites from the Kushtagi-Hungund greenstone belt of the Eastern Dharwar Craton (EDC): implications for the tectonic setting. *Journal of Asian Earth Sciences*, v.27, pp: 25-44.
- Okudaira, T., Hari Prasad, B., and Rajneesh Kumar., 2000. Proterozoic evolution of the Nellore-Khammam schist belt in the Khammam district, SE India. *Jour. Geo. Soc. Osaka city uni.*, v.43, pp: 193-202.
- Pandey, V., Pandey, R.K., and Verma, P.K., 2013. Origin of Amphibolites of Chukru area, Palamau district, Jharkhand, India, *Journal of Applied Geochemistry*, v.15, no.1, pp: 70-77.
- Rogers, A.J., Kolb, J.F., Meyer, M., and Armstrong, R.A., 2007. Tectono-magmatic evolution of the Hutti-Maski Greenstone Belt, India: constrained using geochemical and geochronological data. *Journal of Asian Earth Sciences*, v.31, pp: 55-70.
- Sarvothaman, H., 1995. Amphibolites of Khammam schist belt:evidence for the Precambrian Fe-tholeiitic volcanism in marginal zone. *Indian minerals*, v.49, pp: 177-186.
- Sarvothaman, H., 2001. Archean high-Mg granitoids of mantle origin in the Eastern Dharwar Craton of Andhra Pradesh. *Journal of the Geological Society of India*, v.58, pp: 261-268.
- Sesha Sai, V.V., 2013. Proterozoic Granite Magmatism along the Terrane Boundary Tectonic Zone to the East of Cuddapah basin, Andhra Pradesh – Petrotectonic Implications for Precambrian Crustal Growth in Nellore Schist Belt of Eastern Dharwar Craton, Geological Society of India, Bangalore, v.81, pp: 167-182.
- Sun, S.S., and McDonough, W.F., 1989. Chemical and Isotopic Systematic of Oceanic Basalts: Implication for Mantle Composition and Processes. In: Saunder, A.D. and Norry, M.J., Eds., *Magmatism in the Ocean Basins*, Geological Society, Special Publications, London, v.42, pp: 313-345.
- Thomas, H., and Paudel, L., 2015. Petrogeochemistry of Amphibolites from Shivpuri District Chilvara, Rajasthan, India, *Jour. of Inst of Sci. and Tech*, v.20, no.2, pp: 103-112.
- Van de Camp, P.C., 1969. Origin of Amphibolites in beartooth Mountain, Montana and Wyoming: New Data and Interpretation: *Geological Society of America Bulletin*, v.80, pp: 1127-1136.
- Vijay Kumar, K., Narsimha Reddy, M., and Leelanandam, C., 2006. Dynamic melting of the Precambrian mantle: evidence from rare earth elements of the amphibolites from the Nellore-Khammam Schist Belt, South India. *Contri. Min. and petro.*, pp: 152-243.
- Walker, K.R., Joplin, G.A., Lovering, J.F., and Green, R., 1960. Metamorphic and metasomatic convergence of basic igneous rocks and lime-magnesia sediments of the Pre-Cambrian of northwestern Queensland. *J Geol Soc Australia*, v.6, pp: 147-178.

Received on: 26.11.16; Revised on: 10.2.17; Re-revised on: 3.3.17; Accepted on: 6.3.17